Expansion of T follicular helper cells is associated with disease progression in rat experimental membranous nephropathy model

Li Deng[1,2,C,D], Bishun Deng[1,B,C], Ziling Zhao[1,B], Huijie Huang[1,C], Xiaowan Wang[3,4,B], Ruimin Tian[4,B], Guohua Li[1,B], Enyu Liang[1,B], Anping Peng[1,3,B,C], Peifeng Ke[1,B], Peng Xu[3,4,E,F], Min He[1,3,A,E,F]

[1] Department of Laboratory Medicine, The Second Clinical College of Guangzhou University of Chinese Medicine, China
[2] Department of Laboratory Medicine, Maoming People's Hospital, China
[3] State Key Laboratory of Dampness Syndrome of Chinese Medicine, the Second Affiliated Hospital of Guangzhou University of Chinese Medicine, China
[4] Department of Nephrology, Second Clinical College of Guangzhou University of Chinese Medicine, China

A – research concept and design; B – collection and/or assembly of data; C – data analysis and interpretation;
D – writing the article; E – critical revision of the article; F – final approval of the article

Advances in Clinical and Experimental Medicine, ISSN 1899–5276 (print), ISSN 2451–2680 (online) *Adv Clin Exp Med*. 2024;33(8):889–899

Address for correspondence
Min He
E-mail: minhe@gzucm.edu.cn

Funding sources
1. State Key Laboratory of Dampness Syndrome of Chinese Medicine grant No. SZ2021ZZ24
2. State Key Laboratory of Dampness Syndrome of Chinese Medicine grant No. SZ2021ZZ11
3. Science and Technology Projects in Guangzhou grant No. 202201020334
4. Science and Technology Projects in Guangzhou grant No. 202201020556
5. Science and Technology Projects in Guangzhou grant No. 202201020487
6. GuangDong Basic and Applied Basic Research Foundation grant No. 2020A1515110329
7. Science and technology research project of traditional Chinese Medicine of Guangdong Provincial Hospital of Chinese Medicine grant No. YN2018ML04

Conflict of interest
None declared

Received on October 19, 2023
Reviewed on March 1, 2024
Accepted on June 19, 2024
Published online on August 28, 2024

Cite as
Deng Li, Deng B, Zhao Z, et al. Expansion of T follicular helper cells is associated with disease progression in rat experimental membranous nephropathy model. *Adv Clin Exp Med*. 2024;33(8):889–899. doi:10.17219/acem/189865

DOI
10.17219/acem/189865

Abstract

Background. T follicular helper (Tfh) cells drive humoral immunity by facilitating B cell responses, but the functional role of Tfh cells in the pathogenesis of idiopathic membranous nephropathy (IMN) remains unclear.

Objectives. This study aimed to establish a rat experimental membranous nephropathy model, investigate the phenotypic characteristics of Tfh cells, and analyze a clinically significant correlation between Tfh cells.

Materials and methods. Passive Heymann nephritis (PHN) rats were induced by immunizing Sprague Dawley rats with anti-Fx1A serum. The frequency of Tfh and B cell subsets was analyzed with flow cytometry (FC). The serum concentration of interleukin-21 (IL-21), the relative mRNA expression levels of IL-21 and B cell lymphoma 6 (Bcl-6) in spleen mononuclear cells (MNCs), and the kidney infiltration of $CD4^+$ T cells and IL-21 were assessed. The potential correlations among these measures were analyzed.

Results. In comparison with the control group, significantly increased percentages of Tfh cells, inducible T cell co-stimulator-positive ($ICOS^+$) Tfh cells, and mRNA expression of Bcl-6 were detected in the spleen of PHN rats. Elevated IL-21 expression was detected in the serum and kidneys. Remarkably, the percentage of splenic $ICOS^+$ Tfh cells was positively correlated with 24 h urine protein concentrations ($r = 0.676$, $p = 0.011$) in PHN rats.

Conclusions. These data indicate that $ICOS^+$ Tfh cells contribute to development of IMN, and they might be potential therapeutic targets for IMN.

Key words: B cells, T follicular helper cells, passive Heymann nephritis, interleukin -21, B cell lymphoma 6

Background

Idiopathic membranous nephropathy (IMN) is a major pathological type of adult nephrotic syndrome.[1,2] Idiopathic membranous nephropathy is now recognized as an autoimmune disease with the identification of the podocyte antigens, which includes thrombospondin type-1 domain-containing 7A (THSD7A) and the M-type receptor for phospholipase A2 (PLA2R).[3] Due to impaired immune tolerance, B cells produce nephritogenic autoantibodies, which bind podocytes to form immune deposits, leading to complement activation and damage to the glomerular basement membrane (GBM), creating a risk of renal failure.[4] In patients with IMN, an increased proportion of circulating plasma cells and oligoclonal expansion of B cells in the renal tissue have been observed.[5,6] These findings, together with the clinical efficacy of B-cell-depleting therapies (rituximab), have highlighted the pathogenic role of B lymphocytes in IMN.[7] Despite these findings, the immunological pathogenesis of IMN has not been fully elucidated.

The germinal center (GC) response is crucial for B cell maturation and the establishment of efficacious protective humoral immunity.[8] T follicular helper (Tfh) cells are a distinct subgroup of T cells, which play an essential role in promoting GC reactions and supporting the differentiation of B cells and antibody production.[9,10] They are characterized by their expression of C-X-C chemokine receptor type 5 (CXCR5), programmed cell death protein 1 (PD-1), inducible T cell co-stimulator (ICOS), and B cell lymphoma 6 (Bcl-6). The ICOS and PD-1 are closely associated with the maintenance and function of Tfh cells.[11] B cell lymphoma 6 is considered the dominant lineage-defining transcription factor for Tfh cells.[12] Additionally, Tfh cells can secrete interleukin (IL)-21, which is a crucial cytokine in the regulation of B cell differentiation, maturation and class switch recombination. Moreover, in addition to lymphoid follicles, resident Tfh cells and circulating Tfh (cTfh) cells have been found in the peripheral blood (PB), and were shown to share functional properties with GC Tfh cells.[13]

Recently, aberrant expression of Tfh cells has been shown to contribute to autoimmune disease development, including multiple sclerosis (MS), systemic lupus erythematosus (SLE) and rheumatoid arthritis (RA).[14–16] A defective Tfh checkpoint profoundly impacts immune responses and promotes pathogenic autoantibody production. Despite the enrichment of Tfh cells reported in the circulation of IMN patients,[17,18] the collaboration between Tfh cells and B cell subsets during the pathogenesis of IMN remains largely unknown.

Objectives

To gain insights into the phenotypic and functional characteristics of Tfh cells in the pathogenesis of IMN, this study employed the rat model of passive Heymann nephritis (PHN).[19] The frequencies of Tfh cells and B cell subpopulations were dynamically monitored during PHN induction. Additionally, the correlation between the frequency of Tfh cells with 24 h urine protein was analyzed.

Materials and methods

Induction of passive Heymann nephritis

Male Sprague Dawley rats were obtained from the Medical Experimental Animal Center of Guangdong Province (Guangzhou, China). The animals were housed in polypropylene cages under pathogen-free conditions with a 12 h light/dark cycle and free access to standard laboratory chow and sterile water. Animal experiments were approved by the institutional animal use committee of Guangdong Provincial Hospital of Chinese Medicine (Guangzhou, China; approval No. 2021081). Induction of the PHN rat model was performed as previously described.[20] After acclimatization for 3 days, animals were randomly divided into 2 groups: the PHN group and the control group. Passive Heymann nephritis rats were injected with sheep-derived anti-Fx1A antiserum (Probetex, Inc., San Antonio, USA) in the tail vein at a dose of 0.5 mL/100 g. Rats in the control group were given an equivalent volume of saline. The onset of nephritis in the rats was monitored by assessment of 24 h urine protein. Animals were divided into 5 groups according to the number of days after immunization, with 5 rats in each group. All animals were euthanized on day 0, 2, 6, 13, or 20, and urine, peripheral blood, kidney, and spleen specimens were collected.

Isolation of mononuclear cells from the spleen and peripheral blood

Following euthanasia, blood samples and spleens were harvested from PHN rats and control rats. Blood samples anticoagulated with ethylene diamine tetraacetic acid (EDTA-K2) were collected to separate peripheral blood mononuclear cells (PBMCs). The dissected spleens were homogenized with the tip of a syringe plunger. The homogenates were passed through a 70-μm nylon mesh filter (BD Biosciences, Franklin Lakes, USA), and single-cell suspensions were obtained. Mononuclear cells from peripheral blood or spleen were separated using peripheral blood mononuclear cell isolation kits or spleen lymphocyte isolation kits (both from TBD Science, Tianjin, China) for rats, respectively. The isolated mononuclear cells were used for reverse transcription quantitative polymerase chain reaction (RT-qPCR) or flow cytometry (FC) analysis.

Transmission electron microscopy

Rat renal tissues were fixed with 2.5% glutaraldehyde in 0.1 M sodium cacodylate buffer at 4°C for 2 h. After

washing with the same buffer, renal specimens were post-fixed with 1% osmium tetroxide at 4°C for 2 h, dehydrated through immersion in ascending grades of ethanol, and embedded in Epon 812. Ultrathin sections were stained with uranyl acetate and lead citrate and then examined using transmission electron microscopy (TEM; JEM1400 PLUS; Joel Ltd., Akishima, Tokyo, Japan). The thickness of glomerular basement membrane (GBM) in each ultrathin slice was detected using RADIUS software v. 2.0 (EMSIS, Boston, USA).

Flow cytometry

For Tfh cell detection, mononuclear cells were incubated with anti-rat-CXCR5 (Abcam, Cambridge, UK; ab254415) at 4°C for 30 min, followed by staining with goat anti-rabbit IgG-Alexa Fluor 488 (Abcam; ab150077), anti-rat-CD4-BV421 (BD Biosciences; 743088), and anti-rat-ICOS-PE (eBioscience, Thermo Fisher Scientific, Waltham, USA; 12994981) for 30 min at 4°C. For B cell subset phenotyping, the cells were first stimulated with Leukocyte Activation Cocktail (BD Bioscience) for 6 h, then stained with anti-rat-CD45R-PE-Cyanine7 (Invitrogen, Waltham, USA; 25046082), anti-rat-CD3-APC (Invitrogen; 17003082) and anti-rat-CD27-PE (Invitrogen; 12027182). After cell surface staining, the cells were fixed, permeabilized and stained with anti-rat-IgG-BV605 (BioLegend, San Diego, USA; 405430). Cells were analyzed with the Agilent NovoCyte flow cytometer, and the data were analyzed with Agilent software v. 1.5.6 (Agilent Technologies, Palo Alto, USA).

ELISA

Serum concentrations of IL-21 were measured using a rat enzyme-linked immunosorbent assay (ELISA) kit (Cloud-clone SEB688Ra; Cloud-CloneCorp, Wuhan, China) following the manufacturer's instructions.

Urine analysis

The concentration of urine creatinine and 24 h urine protein was analyzed using Cobas 8000 analyzer (Roche Diagnostics, Mannheim, Germany).

Immunohistochemistry

For immunohistochemical staining, 3 micrometers of serially sliced kidney tissue were used. Paraffin-embedded sections were first deparaffinized and then hydrated. After antigen retrieval, the activity of endogenous peroxidase and non-specific binding sites were blocked. Incubation with mouse anti-CD4 (Immunoway, Plano, USA) or rabbit anti-IL-21 (Affbiotech, Changzhou, China) overnight at 4°C was then performed. Next, sections were incubated with an horseradish peroxidase (HRP)-labeled secondary antibody (Maxin, Fuzhou, China). Finally, the sections were developed in diaminobenzidine solution and counterstained with hematoxylin. Immunostained slides were observed under a fluorescence microscope (BX61; Olympus Corp., Tokyo, Japan). The CD4- and IL-21-positive regions were quantitatively detected using ImageJ software (National Institutes of Health, Bethesda, USA), and these values were described as average optical density (AOD).

Reverse transcription-quantitative PCR

Total RNA from rat spleen mononuclear cells was purified with the Trizol reagent (Invitrogen). After treatment with DNase I, mRNAs were reverse transcribed using Evo M-MLV RT Mix Kit (Accurate Biology, Changhsha, China). The PCR was performed with a SYBR Green PCR Kit (Accurate Biology) on the ViiA7 detection system (Applied Biosystems, Darmstadt, Germany). The sequences of the primers were:
β-actin forward: 5'-GACATGCCGCCTGGAGAAAC-3';
β-actin reverse: 5'-AGCCCAGGATGCCCTTTAGT-3';
IL-21 forward:
5'-GCCAAACTCAAGCCATCAAACACTG-3';
IL-21 reverse: 5'-CTTAGCAGGCAGCCTCCTCCTC-3';
Bcl-6 forward: 5'-TCGAGGTCGTGAGGTTGTGGAG-3';
Bcl-6 reverse: 5'-TCGGATAAGAGGCTGGTGGTGTC-3'.

Gene expression was normalized against β-actin, and the relative expression levels were calculated with the $2^{-\Delta\Delta Ct}$ method.

Statistical analyses

All statistical analyses were performed with the IBM SPSS v. 20.0 software (IBM Corp., Armonk, USA) and GraphPad Prism v. 9.0 software (GraphPad Software Inc., San Diego, USA). Data were collected from independent samples to examine the differences between PHN rats. All variables were performed using nonparametric tests: the Mann–Whitney U test was used for comparison between the 2 groups, and the Kruskal–Wallis with Bonferroni correction for multiple testing was used for comparisons between 3 or more groups. The data were expressed as median ± interquartile range (±IQR), and correlations were determined using Spearman's correlation coefficients. A p-value <0.05 was considered statistically significant.

Results

Pathologic changes of nephritic function in PHN rats induced by anti-Fx1A antiserum

Twenty days after administration of the anti-Fx1A antibody, the GBM was irregularly thickened. In addition, subepithelial electron-dense deposits were observed, and characteristic spike-like structures were formed in PHN rats (Fig. 1A). Quantitative analysis of TEM results (Fig. 1B)

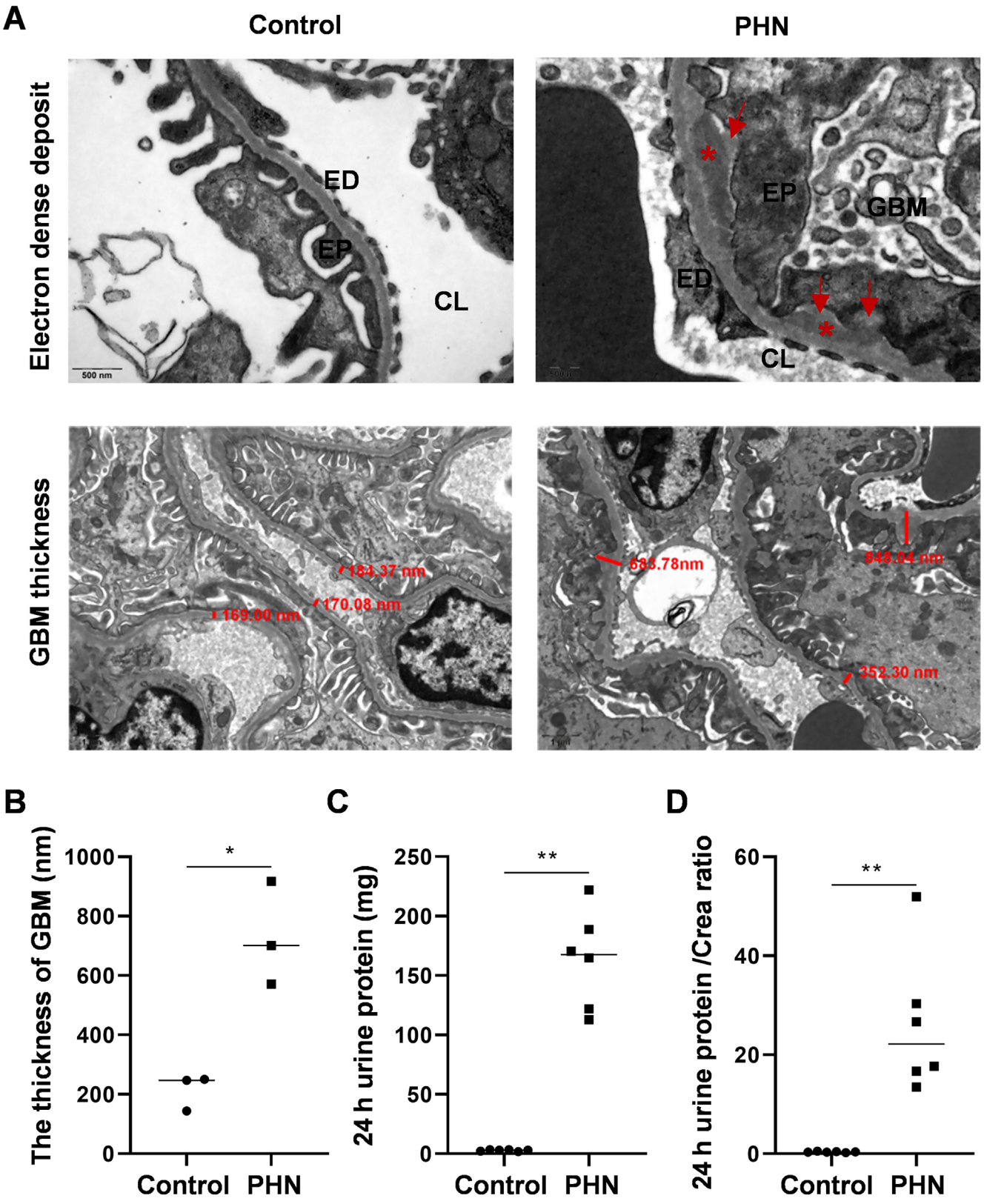

Fig. 1. Pathologic change of nephritic function in passive Heymann nephritis (PHN) rats. The animals were induced with anti-Fx1A antiserum. A. Transmission electron micrograph (TEM) of the glomerular capillary wall from control and PHN rats at 20 days after anti-Fx1A antiserum injection. The red asterisks indicate electron-dense deposits, and the red arrows represent the new basement membrane (TEM × 30,000 and × 12,000, respectively). B. Comparison of semi-quantification of GBM thickness in control and PHN rats (n = 3); C,D. Comparison of 24 h urine protein (C) and 24 h urine protein/creatinine ratio (D) in control and PHN rats (n = 6 for each). Horizontal line shows the median. *$p < 0.05$ and **$p < 0.01$ using Mann–Whitney U test

GBM – glomerular basement membrane; EP – epithelial cell; ED – endothelial cell; CL – capillary lumen.

showed the thickness of GBM in PHN rats was significantly greater than in control rats (701.6 ±172.8 nm vs 247.0 ±53.4 nm, Mann–Whitney U test, p = 0.05). In addition, PHN rats developed significantly heavier proteinuria, as evidenced by increased 24 h urine protein (167.7 ±77.4 mg vs 3.0 ±1.4 mg, Mann–Whitney U test, p = 0.004; Fig. 1C) and the 24 h urine protein/creatinine ratio (Mann–Whitney U test, p = 0.004; Fig. 1D). These results suggest that PHN rats developed nephritis after immunization with anti-Fx1A antiserum.

Tfh cells were expanded and activated in the spleen in PHN rats

We then examined whether Tfh (defined as $CD4^+CXCR5^+$) cells were enriched in the context of rat PHN models. Both circulating and splenic Tfh cells were characterized employing FC analysis. The gating strategy and representative plots are shown in Fig. 2A–C. On day 20 following immunization with anti-Fx1A antibody, phenotypic analysis indicated the percentages of Tfh cells among splenic MNCs (Mann–Whitney U test, p = 0.025; Fig. 2D, left) and $CD4^+$ T cells were significantly higher in PHN rats than the control group (Mann–Whitney U test, p = 0.016; Fig. 2E, left). Similarly, an approximately twofold increase in $ICOS^+$ Tfh cells in splenic $CD4^+$ T cells was observed in PHN rats as compared to control rats (0.34 ±0.3% vs 0.19 ±0.08%, Mann–Whitney U test, p = 0.016; Fig. 2F, left). However, varying expression patterns were observed concerning circulating Tfh cells, which were considered peripheral memory Tfh cells. Although higher frequencies of circulating Tfh cells among MNCs or $CD4^+$ T cells were found in PHN rats as compared to the control group, no significant difference was observed (Fig. 2D–F, right). In addition, circulating $ICOS^+$ Tfh cells were comparable between the 2 groups. Therefore, $ICOS^+$ Tfh cells were enriched in the spleen but not in the PB of PHN rats.

Distribution of B cell subsets in PHN rats

To investigate the association between dysregulation of Tfh cells and B cells, we subsequently examined splenic B cell subsets in PHN rats. Among the B cell subsets, total B cells ($CD3^-CD45R^+$), antibody-secreting B cells (ASCs, defined as $CD3^-CD45R^+IgG^+$), and memory B cells ($CD3^-CD45R^+CD27^+$) were evaluated. In agreement with a previous study,[21] no statistical difference in the frequency of total B cells was observed 20 days after immunization (Mann–Whitney U test, p = 0.513). However, there was a significant induction of ASCs (Mann–Whitney U test, p = 0.05) and a reduction of memory B cells (Mann–Whitney U test, p = 0.05) in PHN rats compared to control rats (Fig. 3A–E). Moreover, as shown in Fig. 3F–H, kinetic analysis showed distinct differentiation patterns of B cell subsets over the immunization time. Of note, rapid induction of total B cells was identified on day 2 (Kruskal–Wallis with Bonferroni correction, day 2 vs day 0, p = 0.031) and then gradually decreased. The frequency of IgG^+ ASCs was continually increased, reaching a peak at day 20. Therefore, the B cell subset was found to be altered, which may affect autoantibody production in IMN disease.

Dynamic changes of Tfh cell frequency in PHN rats and the correlation with disease progression

To obtain a deeper insight into the role of Tfh cells in IMN development, we dynamically monitored the changes in Tfh cells and Bcl-6 expression in the spleen of PHN rats. Consistent with progressive development of nephritis (Fig. 1), the proportion of Tfh cells showed an increasing trend during the development of PHN, which reached a peak at day 13 (Kruskal–Wallis test with Bonferroni correction, day 13 vs day 0, p = 0.019, Fig. 4A). A rapid induction of $ICOS^+$ Tfh cells was found on day 2, remaining stable through day 20 (Fig. 4B). Bcl-6 is a key transcription factor for the programming of Tfh cells. The RT-qPCR also confirmed the mRNA level of Bcl-6 in spleen MNCs of PHN rats was elevated (Kruskal–Wallis with Bonferroni correction, day 6 vs day 0, p = 0.006; Fig. 4C). In addition, although no significant correlation was found between the frequency of Tfh cells and 24 h urine protein, the percentage of $ICOS^+$ Tfh cells and Bcl-6 mRNA levels were positively associated with 24 h urine protein levels (r = 0.676, p = 0.011; r = 0.706, p = 0.034, respectively) (Fig. 4D–F). Taken together, these results suggest that an induction of Tfh cells was accompanied by the progression of PHN.

The expression of IL-21 was elevated in PHN rats

Interleukin-21 is reported to be the main effector of Tfh cells; thus, we next explored its expression in PHN rats. As shown in Fig. 5A, serum concentrations of IL-21 began to rise on day 2 and peaked on day 13 after immunization (Kruskal–Wallis test with Bonferroni correction, day 13 vs day 0, p = 0.041). Consistent with this finding, IL-21 mRNA expression in spleen MNCs was higher, but not significantly, in PHN rats than in control rats (Fig. 5B). Furthermore, IHC was performed to compare expression and localization of $CD4^+$ and $IL\text{-}17^+$ cells in kidney tissue from PHN and control rats. As shown in Fig. 5C–E, the infiltration of $IL\text{-}21^+$ cells and $CD4^+$ cells was significantly increased in the kidney tissue of PHN rats than control rats, especially around the kidney tubules (Fig. 5C). Passive Heymann nephritis rats showed a significantly higher AOD value of CD4 (0.237 ±0.007 vs 0.231 ±0.009, Mann–Whitney U test, p = 0.047; Fig. 5D) and IL-21 (0.292 ±0.008 vs 0.287 ±0.004, Mann–Whitney U test, p = 0.047; Fig. 5E). These results confirmed IL-21 was elevated in PHN rats.

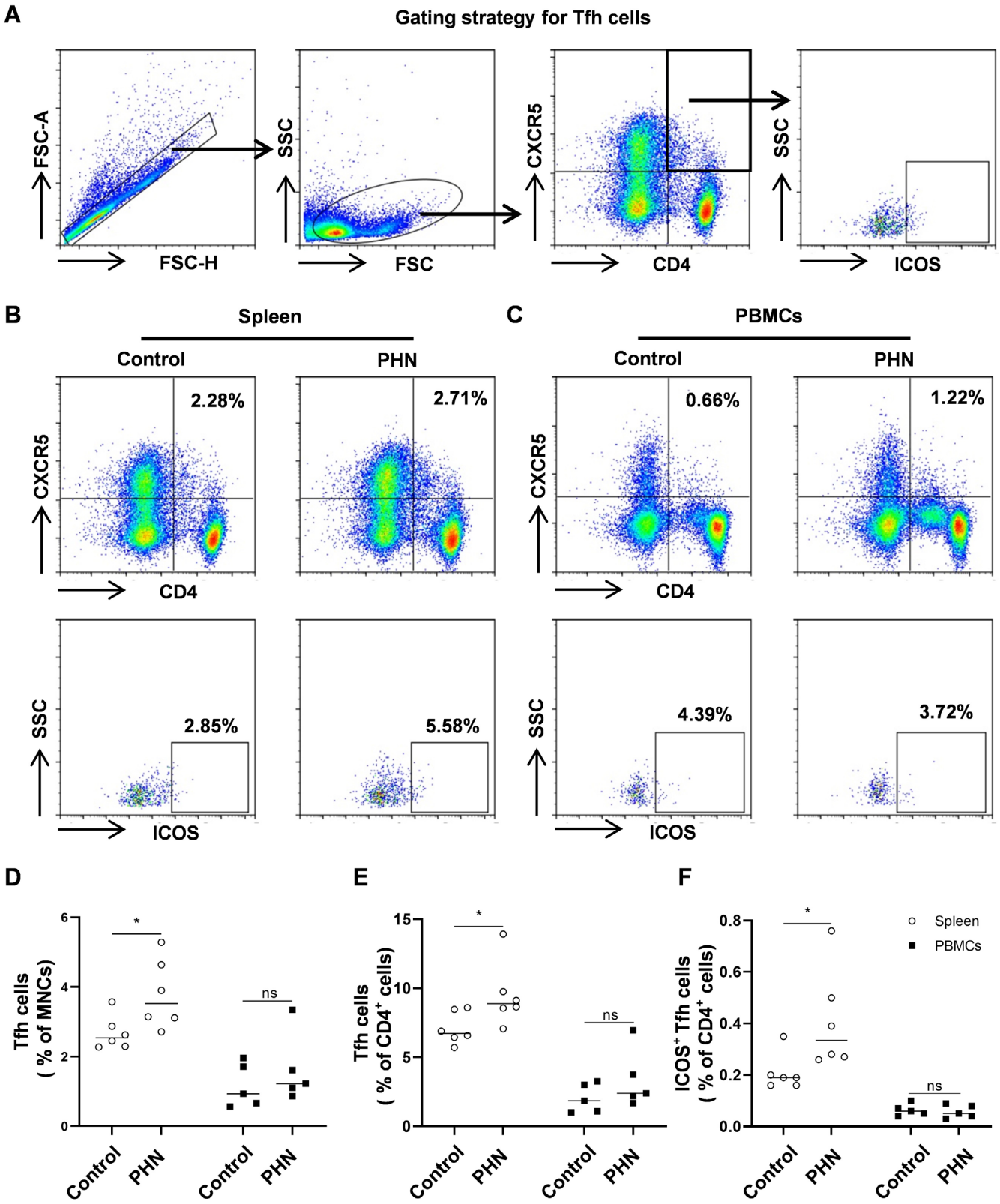

Fig. 2. T follicular helper (Yfh) cells were expanded in the spleen of passive Heymann nephritis (PHN) rats. The PHN and control rats were euthanized on day 20, mononuclear cells (MNCs) were separated from peripheral blood and spleen, and Tfh cell subpopulations were detected using flourescence activated cell sorting (FACS). A. Gating strategy for Tfh cell subsets; B,C. Representative flow cytometric histograms for inducible T cell co-stimulator-positive ($ICOS^+$) Tfh cells in spleen (B) and peripheral blood mononuclear cells (PBMCs) (C) from control and PHN rats; D–F. Statistical analysis of the frequencies of Tfh cells of MNCs (D), Tfh cells of $CD4^+$ cells (E) and $ICOS^+$ Tfh cells (F) between control and PHN rats, n = 5 of each. Significant differences were assessed with Mann–Whitney U test

Horizontal line shows median; NS – not significant; *$p < 0.05$.

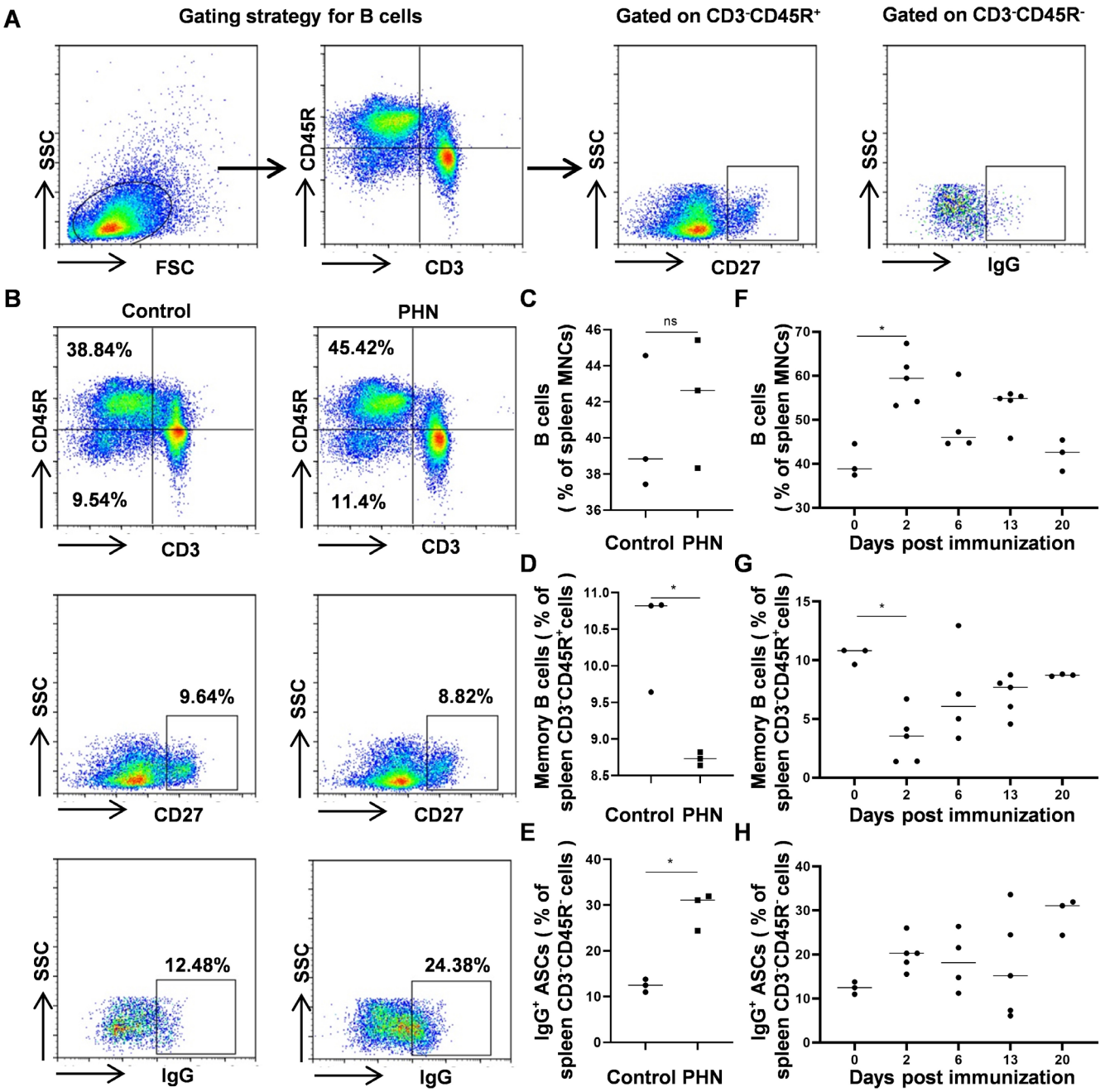

Fig. 3. The frequency of B cells in passive Heymann nephritis (PHN) rats. The B cell subpopulations of control and PHN rats were detected in spleen mononuclear cells (MNCs), and their correlation with different T cell subsets was analyzed. A,B. Gating strategy (A) and representative plots (B) of B cell subpopulations analyzed using flourescence activated cell sorting (FACS); C–E. Statistical analysis of the percentage of B cells (C), memory B cells (D) and IgG$^+$ ASCs (E) in control and PHN rats (n = 3 for each). Significant differences were assessed with Mann–Whitney U test. *p < 0.05 compared with control rats; F–H. The kinetic frequency of B cells (F), memory B cells (G) and IgG$^+$ ASCs (H) in B cells at indicated times. Significant differences were assessed using Kruskal–Wallis with Bonferroni correction

Horizontal line shows median; *p < 0.05 compared with PHN rats euthanized on day 0; NS – not significant.

Discussion

T follicular helper cells are crucial regulators of GC formation, B cell development and long-term memory responses.[22] In this study, we report that Tfh cells are highly enriched and activated in PHN rats, and their frequency is significantly associated with disease severity.

The PHN model is a classical model for investigating the pathogenesis of IMN. In this study, the PHN rats displayed histopathological and laboratory features of IMN, including irregularly thickened GBM, subepithelial spikes on the outer surface of the capillary wall, abnormal proteinuria development, and an elevated 24 h urine protein/creatinine ratio. Dynamic results suggested that splenic

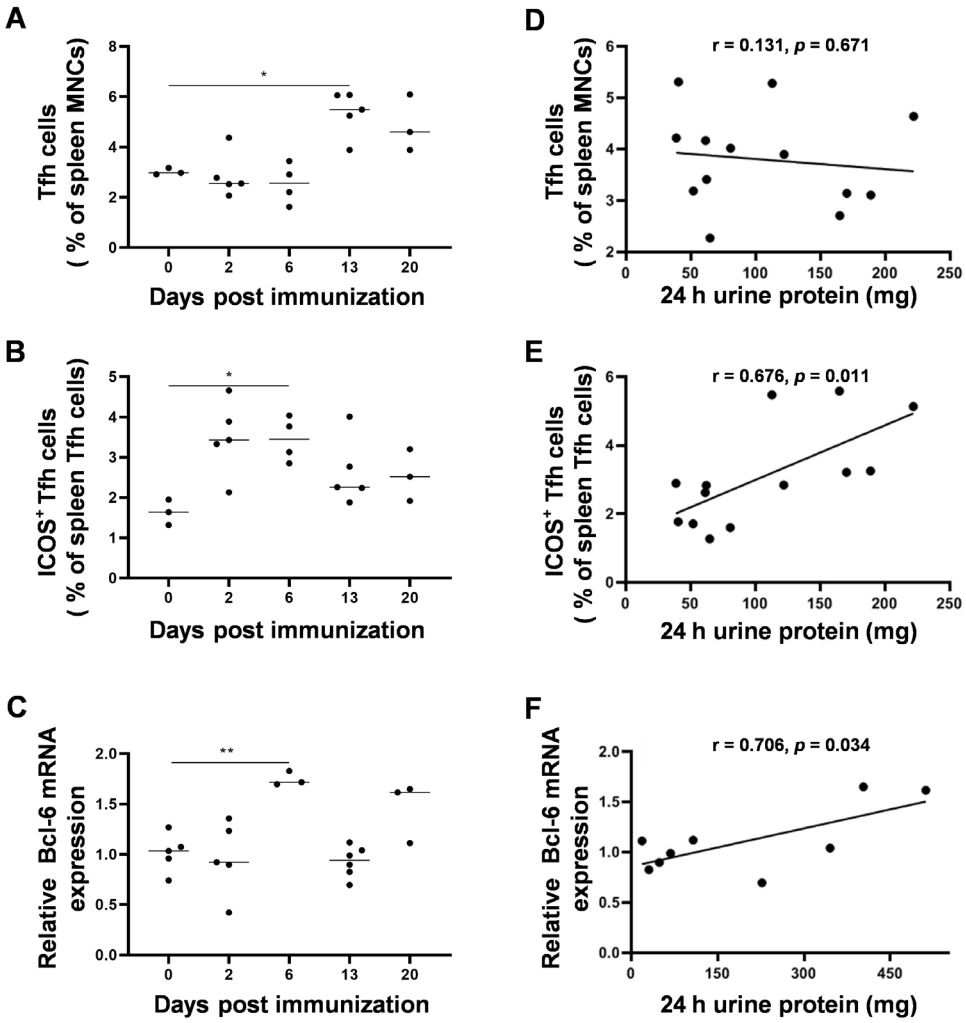

Fig. 4. Dynamic changes of activated T cell frequency in passive Heymann nephritis (PHN) rats and correlation with disease progression. Passive Heymann nephritis rats were euthanized on day 0, 2, 6, 13, or 20, and spleen mononuclear cells (MNCs) were separated for flourescence activated cell sorting (FACS) analysis and reverse transcription quatitative polymerase chain reaction (RT-qPCR), while 24 h urine samples were collected for 24 h urine protein detection. A,B. The kinetic detection of the frequency of T follicular helper (Tfh) cells (A) and inducible T cell co-stimulator-positive (ICOS+) Tfh cells (B) at specific days as indicated (n ≥ 3 for each); C. Fold change of B cell lymphoma 6 (Bcl-6) mRNA in PHN rats; D–E. Correlation of 24 h urine protein with the frequency of Tfh cells (D) and ICOS+ Tfh cells (E) in PHN rats (n = 13 for each); F. Association of 24 h urine protein with the fold change of Bcl-6 mRNA (n = 9). Horizontal line shows the median, with *p < 0.05, **p < 0.01 using Kruskal–Wallis with multiple comparisons of Bonferroni correction (A–C). Spearman correlation statistics are shown in D–F

Tfh cells were gradually upregulated after injection with anti-Fx1A antiserum and were significantly higher than in the control group on day 20. Additionally, RT-qPCR results also indicated that Tfh cells upregulated Bcl-6, which is a specific transcription factor for Tfh cell differentiation.[23,24] These findings demonstrated that splenic Tfh cells were mature in PHN rats. It is noteworthy that Zhang et al. previously reported an expansion of cTfh cells in patients with IMN.[17] However, despite higher frequencies of circulating Tfh cells found in PHN rats, no significant difference was found between those and the control group. This discrepancy may be representative of the different stages of disease. In this study, circulating Tfh cells were induced at the onset of disease, which preceded the appearance of proteinuria, whereas in Zhang et al. elevated cTfh cells were found in confirmed IMN patients with kidney injury and high proteinuria. Consistent with our results, the induction of Tfh cells was found in the lymph node biopsies of early RA patients, whereas the frequency of Tfh cells did not differ in the blood between RA patients and controls.[25] In particular, mass cytometric comparison results have suggested that cTfh cells can be generated at the T cell–B cell border, and then travel through efferent lymph to the blood.[26,27] Overall, these results confirmed that Tfh cells are expanded in the PHN model and the elevation of Tfh cells were fist detected in the spleen but not in the PB after immunization.

Splenic Tfh cells from PHN rats expressed higher ICOS than the control group, whereas no significant differences were found in the frequency of circulating ICOS+ Tfh cells. Interestingly, the correlation analysis indicated that splenic ICOS+ Tfh cells, together with the Bcl-6 mRNA levels, positively correlated with concentrations of 24 h urine protein, which was the clinical biomarker for monitoring disease severity. In particular, several studies showed an offset between immunologic and clinical remissions that was indicative of the longer timespan needed to form enough deposits to initially induce proteinuria and the time needed to remove subepithelial deposits, repair podocyte and capillary wall damage, and restore glomerular perm selectivity.[28] These data suggested that higher percentages of Tfh cells, especially ICOS+ Tfh cells, may be considered as a potential biomarker to monitor the disease activity of IMN.

Interleukin-21, a pleiotropic Tfh cell-derived cytokine, has been proven to play a crucial role in the formation and

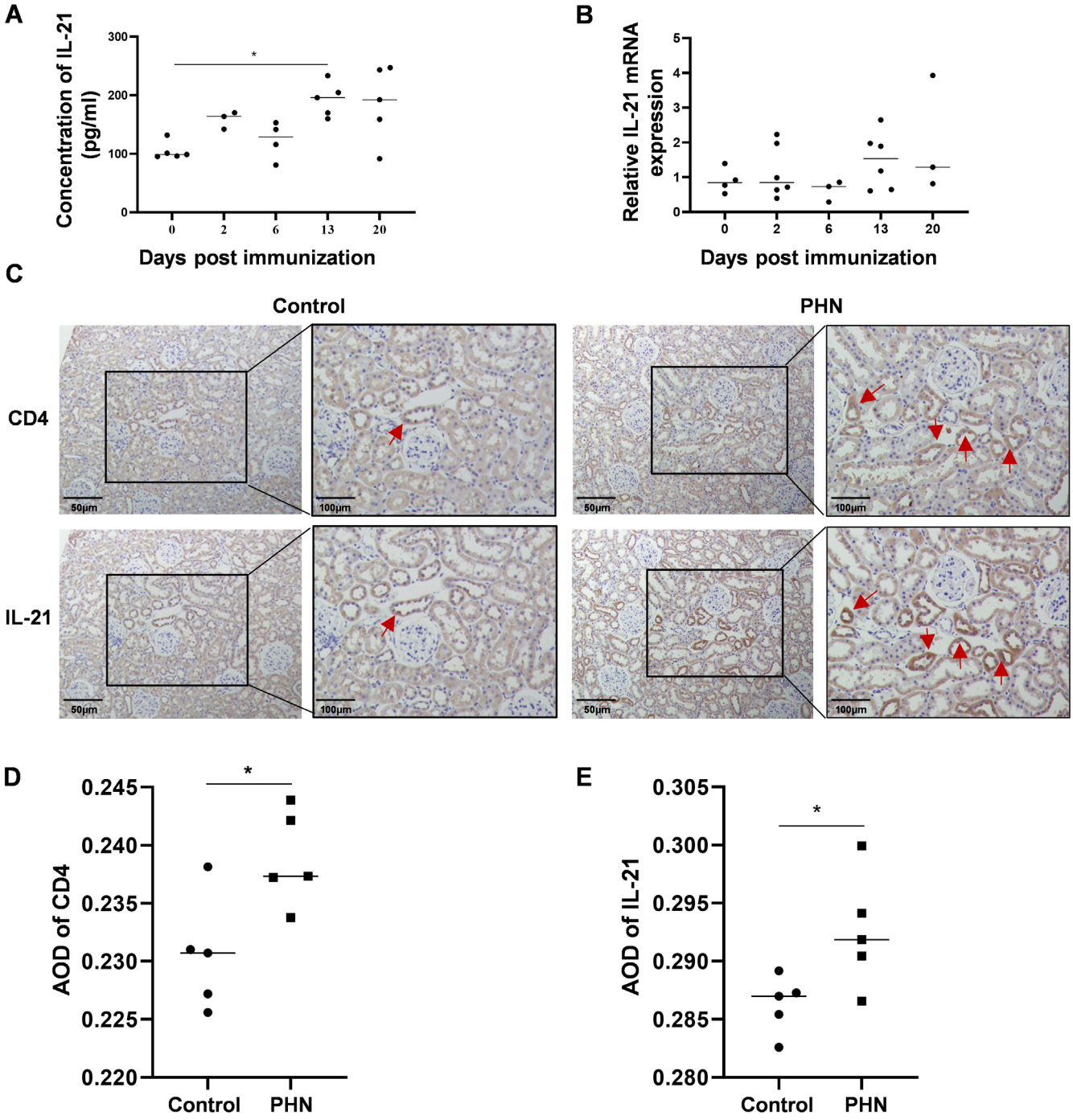

Fig. 5. The expression of interleukin (IL)-21 was elevated in passive Heymann nephritis (PHN) rats. The serum concentration, relative mRNA expression and kidney infiltration of IL-21 were detected in PHN rats. A,B. The serum concentration of IL-21 (A) and fold change of IL-21 mRNA (B) in PHN rats; C–E. Expression level of CD4 and IL-21 in control and PHN rats detected with immunohistochemistry (IHC). The right panels show higher-magnification views of the box area (C). Red arrow shows the positive cell staining. Scale bars represent 50 μm or 100 μm, respectively. ImageJ software was used to quantify IHC results, and values were expressed as average optical density (AOD). Statistical analysis AOD of CD4 (D) and IL-21 (E) in control and PHN rats (n = 5 for each). Horizontal line shows the median. *$p < 0.05$ using Kruskal–Wallis with multiple comparisons test of Bonferroni correction (A and B) and Mann–Whitney U test (D and E)

maintenance of germinal centers (GCs), as well as the development of B cells. Thus, the expression of IL-21 was intensively investigated. Due to a lack of directly labeled FC antibodies for rat IL-21, we used 3 methods to detect IL-21 levels instead. First, kinetic analysis indicated that serum IL-21 began to increase on day 2 after immunization, which was before the manifestation of proteinuria. Second, RT-qPCR results showed that relative expression levels of IL-21 mRNA in PHN group exhibited a rising trend, although they were not statistically significant as compared to the control group (Fig. 5B). Moreover, elevated IL-21$^+$ cells and CD4$^+$ cells were observed in the kidney tissue of PHN rats as opposed to control rats. Also, successive sections of IHC results demonstrated that IL-21 and CD4

signals were detected in the same location (Fig. 5C–E). In addition, our previous study confirmed elevated serum IL-21 expression in IMN patients compared to healthy controls.[29] Thus, our data demonstrated that the expression of IL-21 was elevated in PHN rats, which might be a new clinical biomarker for monitoring disease processes.

It is widely accepted that the expansion of Tfh cells leads to perturbations of B cells that could eventually contribute to the development of autoimmune disorders.[30] As such, we take an interest in B cell subset distribution and the association between B cell subsets and Tfh cells in IMN. Interestingly, the distribution of B cell subsets was different. The antibody producing ASCs were expanded, but the memory B cells were decreased in PHN rat spleens compared with the normal group (Fig. 3D,E). Memory B cells are located in the blood, spleen and other lymphoid organs and are a critical reservoir for plasma cell generation in the secondary response.[31] This reduction of memory B cells might be a result of their differentiation into antibody-producing ASCs. Consistent with our results, a reduction of circulating memory B cells in IMN patients has been reported.[21]

Limitations

The lack of rat antibodies restricted our ability to sort Tfh cells and further characterize the helper function of B cells in PHN rats. Additionally, negative feedback between T and B cells has been reported. In patients with MS, activated memory B cells can suppress the proliferation of Tfh cells.[32] Therefore, further research is required to define the mechanisms of T cells and B cells collaboration in the promotion of disease progression.

Conclusions

Altogether, our study confirmed that Tfh cells and ASCs were significantly increased in PHN rats. Furthermore, Tfh cells were activated by upregulating ICOS and IL-21 expression, and the frequency of $ICOS^+$ Tfh cells was positively correlated with 24 h urine protein. These findings document the importance of Tfh cells in the pathogenesis of IMN and provide a potential new therapeutic target.

Supplementary data

The Supplementary materials are available at https://doi.org/10.5281/zenodo.11406851. The package includes the following files:

Supplementary Table 1. Comparing parameters between controls and PHN rats.

Supplementary Fig. 1. Isotype control staining results for IHC.

Supplementary Fig. 2. Statistical analysis for data in PHN rats.

Data availability

The datasets generated and/or analyzed during the current study are available from the corresponding author on reasonable request.

Consent for publication

Not applicable.

ORCID iDs

Li Deng https://orcid.org/0000-0002-0873-0388
Bishun Deng https://orcid.org/0000-0002-2579-3380
Ziling Zhao https://orcid.org/0000-0002-3995-2872
Huijie Huang https://orcid.org/0000-0002-1286-2252
Xiaowan Wang https://orcid.org/0000-0001-9152-8908
Ruimin Tian https://orcid.org/0000-0001-8591-9419
Enyu Liang https://orcid.org/0000-0002-3499-503X
Anping Peng https://orcid.org/0000-0001-5668-4323
Peng Xu https://orcid.org/0000-0003-0048-8723
Min He https://orcid.org/0000-0003-0361-8984

References

1. Ronco P, Debiec H. Molecular pathogenesis of membranous nephropathy. *Ann Rev Pathol Mech Dis*. 2020;15(1):287–313. doi:10.1146/annurev-pathol-020117-043811
2. Ronco P, Beck L, Debiec H, et al. Membranous nephropathy. *Nat Rev Dis Primers*. 2021;7(1):69. doi:10.1038/s41572-021-00303-z
3. Liu W, Gao C, Dai H, et al. Immunological pathogenesis of membranous nephropathy: Focus on PLA2R1 and its role. *Front Immunol*. 2019;10:1809. doi:10.3389/fimmu.2019.01809
4. Lateb M, Ouahmi H, Payré C, et al. Anti-PLA2R1 antibodies containing sera induce in vitro cytotoxicity mediated by complement activation. *J Immunol Res*. 2019;2019:1324804. doi:10.1155/2019/1324804
5. Cantarelli C, Jarque M, Angeletti A, et al. A comprehensive phenotypic and functional immune analysis unravels circulating anti-phospholipase A2 receptor antibody secreting cells in membranous nephropathy patients. *Kidney Int Rep*. 2020;5(10):1764–1776. doi:10.1016/j.ekir.2020.07.028
6. Kolovou K, Laskari K, Roumelioti M, et al. B-cell oligoclonal expansions in renal tissue of patients with immune-mediated glomerular disease. *Clin Immunol*. 2020;217:108488. doi:10.1016/j.clim.2020.108488
7. Fervenza FC, Appel GB, Barbour SJ, et al. Rituximab or cyclosporine in the treatment of membranous nephropathy. *N Engl J Med*. 2019;381(1):36–46. doi:10.1056/NEJMoa1814427
8. Olatunde AC, Hale JS, Lamb TJ. Cytokine-skewed Tfh cells: Functional consequences for B cell help. *Trends Immunol*. 2021;42(6):536–550. doi:10.1016/j.it.2021.04.006
9. Crotty S. T follicular helper cell differentiation, function, and roles in disease. *Immunity*. 2014;41(4):529–542. doi:10.1016/j.immuni.2014.10.004
10. Song W, Craft J. T follicular helper cell heterogeneity: Time, space, and function. *Immunol Rev*. 2019;288(1):85–96. doi:10.1111/imr.12740
11. Shi J, Hou S, Fang Q, Liu X, Liu X, Qi H. PD-1 controls follicular T helper cell positioning and function. *Immunity*. 2018;49(2):264–274.e4. doi:10.1016/j.immuni.2018.06.012
12. Choi J, Crotty S. Bcl6-mediated transcriptional regulation of follicular helper T cells (TFH). *Trends Immunol*. 2021;42(4):336–349. doi:10.1016/j.it.2021.02.002
13. Morita R, Schmitt N, Bentebibel SE, et al. Human blood $CXCR5^+CD4^+$ T cells are counterparts of T follicular cells and contain specific subsets that differentially support antibody secretion. *Immunity*. 2011;34(1):108–121. doi:10.1016/j.immuni.2010.12.012
14. Rao DA, Gurish MF, Marshall JL, et al. Pathologically expanded peripheral T helper cell subset drives B cells in rheumatoid arthritis. *Nature*. 2017;542(7639):110–114. doi:10.1038/nature20810

15. Zhang X, Ge R, Chen H, et al. Follicular helper CD4$^+$ T cells, follicular regulatory CD4$^+$ T cells, and inducible costimulator and their roles in multiple sclerosis and experimental autoimmune eencephalomyelitis. *Mediators Inflamm*. 2021;2021:2058964. doi:10.1155/2021/2058964
16. Wei X, Niu X. T follicular helper cells in autoimmune diseases. *J Autoimmun*. 2023;134:102976. doi:10.1016/j.jaut.2022.102976
17. Zhang Z, Shi Y, Yang K, Crew R, Wang H, Jiang Y. Higher frequencies of circulating ICOS$^+$, IL-21$^+$ T follicular helper cells and plasma cells in patients with new-onset membranous nephropathy. *Autoimmunity*. 2017;50(8):458–467. doi:10.1080/08916934.2017.1385775
18. Shi X, Qu Z, Zhang L, et al. Increased ratio of ICOS$^+$/PD-1$^+$ follicular helper T cells positively correlates with the development of human idiopathic membranous nephropathy. *Clin Exp Pharmacol Physiol*. 2016;43(4):410–416. doi:10.1111/1440-1681.12555
19. Jiang H, Feng Z, Zhu Z, et al. Advances of the experimental models of idiopathic membranous nephropathy (Review). *Mol Med Rep*. 2020;21(5):1993–2005. doi:10.3892/mmr.2020.11014
20. Wang X, Liu J, Tian R, et al. Sanqi oral solution mitigates proteinuria in rat passive heymann nephritis and blocks podocyte apoptosis via Nrf2/HO-1 pathway. *Front Pharmacol*. 2021;12:727874. doi:10.3389/fphar.2021.727874
21. Rosenzwajg M, Languille E, Debiec H, et al. B- and T-cell subpopulations in patients with severe idiopathic membranous nephropathy may predict an early response to rituximab. *Kidney Int*. 2017;92(1):227–237. doi:10.1016/j.kint.2017.01.012
22. Crotty S. Follicular Helper CD4 T Cells (T_{FH}). *Ann Rev Immunol*. 2011;29(1):621–663. doi:10.1146/annurev-immunol-031210-101400
23. Ciucci T, Vacchio MS, Chen T, et al. Dependence on Bcl6 and Blimp1 drive distinct differentiation of murine memory and follicular helper CD4$^+$ T cells. *J Exp Med*. 2022;219(1):e20202343. doi:10.1084/jem.20202343
24. Liu D, Yan J, Sun J, et al. BCL6 controls contact-dependent help delivery during follicular T-B cell interactions. *Immunity*. 2021;54(10):2245–2255.e4. doi:10.1016/j.immuni.2021.08.003
25. Anang DC, Ramwadhdoebe TH, Hähnlein JS, et al. Increased frequency of CD4$^+$ follicular helper T and CD8$^+$ follicular T cells in human lymph node biopsies during the earliest stages of rheumatoid arthritis. *Cells*. 2022;11(7):1104. doi:10.3390/cells11071104
26. Walker LSK. The link between circulating follicular helper T cells and autoimmunity. *Nat Rev Immunol*. 2022;22(9):567–575. doi:10.1038/s41577-022-00693-5
27. Wong MT, Chen J, Narayanan S, et al. Mapping the diversity of follicular helper T cells in human blood and tonsils using high-dimensional mass cytometry analysis. *Cell Rep*. 2015;11(11):1822–1833. doi:10.1016/j.celrep.2015.05.022
28. Francis JM, Beck LH, Salant DJ. Membranous nephropathy: A journey from bench to bedside. *Am J Kidney Dis*. 2016;68(1):138–147. doi:10.1053/j.ajkd.2016.01.030
29. Liu M, Huang D, Liang E, et al. Elevated plasma interleukin 21 is associated with higher probability and severity of idiopathic membranous nephropathy. *J Lab Med*. 2023;47(3):121–127. doi:10.1515/labmed-2022-0149
30. Crotty S. T follicular helper cell biology: A decade of discovery and diseases. *Immunity*. 2019;50(5):1132–1148. doi:10.1016/j.immuni.2019.04.011
31. Inoue T, Moran I, Shinnakasu R, Phan TG, Kurosaki T. Generation of memory B cells and their reactivation. *Immunol Rev*. 2018;283(1):138–149. doi:10.1111/imr.12640
32. Asashima H, Axisa PP, Pham THG, et al. Impaired TIGIT expression on B cells drives circulating follicular helper T cell expansion in multiple sclerosis. *J Clin Invest*. 2022;132(20):e156254. doi:10.1172/JCI156254